Journal of Taibah University Medical Sciences (2021) 16(2), 162–176

Taibah University

Journal of Taibah University Medical Sciences

www.sciencedirect.com

Original Article

In-silico analysis of the inhibition of the SARS-CoV-2 main protease by some active compounds from selected African plants

Haruna I. Umar, HND [a,*], Sunday S. Josiah, MTech [a], Tolulope P. Saliu, MSc [a], Tajudeen O. Jimoh, MTech [b], Adeola Ajayi, BSc [a] and Jamilu B. Danjuma, PGD [c]

[a] *Department of Biochemistry, Federal University of Technology, Akure, Ondo State, Nigeria*
[b] *Faculty of Pharmaceutical Sciences, Department of Pharmacognosy and Pharmaceutical Botany, Chulalongkorn University, Bangkok, Thailand*
[c] *Department of Biochemistry and Molecular Biology, Federal University, Birnin Kebbi, Kebbi State, Nigeria*

Received 18 September 2020; revised 28 November 2020; accepted 13 December 2020; Available online 6 January 2021

الملخص

أهداف البحث: على مر السنين، أثبتت أزاديراشتا إنديكا، مانجيفيرا إنديكا وموارينجا أوليفيرا أن لديهم بعض الخصائص المضادة للفيروسات. تطبق هذه الدراسة تقنيات الالتحام الجزيئي لتقييم الآثار المثبطة لبعض المركبات البيولوجية النشطة من النباتات المذكورة أعلاه ضد الإنزيم البروتيني الرئيس، وهو البروتين الرئيس المتضمن في تكاثر فيروس سارس-كوفيد-٢. وعلاوة على ذلك، تم توقع فحص المركبات للكشف عن الامتزاز والتوزيع والتمثيل الغذائي والإفراز والسمية في السيليكو.

طرق البحث: تم الحصول على التركيب البلوري للإنزيم البروتيني الرئيس من قاعدة بيانات البروتين، بينما تم الحصول على المركبات البيولوجية النشطة من الكيمياء المنشورة. وتم تقييم تشابه الأدوية للمركبات المختارة ودواء التحكم (الهيدروكسيكلوروكوين). كما تمت ترسية المركبات المطابقة لقاعدة الأدوية المشابهة ضد الإنزيم البروتيني الرئيس، وتم تحليل المجمع الرأسي باستخدام خدمة التعريف ليج بلوت والبروتين المجند. تعرضت أفضل خمس مركبات ناجحة إلى فحص الامتزاز والتوزيع والتمثيل الغذائي والإفراز والسمية باستخدام معرف سار ادمت.

النتائج: ١٧ من ٢٢ من المركبات التي تم فحصها اجتازت تقييم ليبينسكي. بالإضافة إلى ذلك، أظهرت أكثر المركبات نشاطا من النباتات التي تم فحصها إمكانات مثبطة نسبيا ضد الإنزيم البروتيني الرئيس عند مقارنتها بالهيدروكسيكلوروكوين، الأمر الذي يلمح إلى مشاركتهم المحتملة في تثبيط عملية التكاثر للإنزيم البروتيني الرئيس لفيروس سارس-كوفيد-٢.

الاستنتاجات: في هذه الدراسة، معظم المكونات النباتية النشطة عرضت إمكانات مثبطة ضد الإنزيم البروتيني الرئيس لفيروس سارس-كوفيد-٢ والخصائص الدوائية المفضلة عند مقارنتها بالهيدروكسيكلوروكوين، مما يجعلها مضادات محتملة للفيروسات ضد مرض فيروس كورونا.

الكلمات المفتاحية: أزاديراشتا إنديكا؛ في السيليكو مانجيفيرا إنديكا؛ مورينجا أوليفيرا؛ الإنزيم البروتيني الرئيس لفيروس سارس-كوفيد-؛ ٢

Abstract

Objectives: Over the years, *Azadirachta indica, Mangifera indica,* and *Moringa oleifera* have been shown to possess some antiviral characteristics. This study applies molecular docking techniques to assess inhibitory effects of some bioactive compounds from the plants mentioned above against the main protease (Mpro), a key protein involved in SARS-CoV-2 replication. Furthermore, adsorption, distribution, metabolism, excretion, and toxicity (ADMET) profiles for screened compounds were predicted *in silico*.

Methods: The crystal structure of Mpro was retrieved from the Protein Data Bank, while the plant bioactive compounds were retrieved from Pubchem. Drug-likeness of the selected compounds and a control drug (hydroxychloroquine) were assessed, and the compounds that satisfied the drug-likeness rule were docked against Mpro. The docked complexes were analyzed using LigPlot and the protein-ligand profiler server. The top five compound hits were subjected to ADMET screening using the ADMETSar server.

Results: A total of 17 out of 22 screened compounds passed Lipinski's assessment. Additionally, the most

* Corresponding address: Department of Biochemistry, Federal University of Technology, Along Owo-Ilesha Express way, P.M.B. 704, Akure, Ondo State, Nigeria.
E-mail: ariwajoye3@gmail.com (H.I. Umar)

Peer review under responsibility of Taibah University.

ELSEVIER Production and hosting by Elsevier

 https://doi.org/10.1016/j.jtumed.2020.12.005

active compounds from the investigated plants exhibited relative inhibitory potentials against Mpro compared with hydroxychloroquine, which alludes to their possible involvement in inhibiting the SARS-CoV-2 main protease replication process.

Conclusions: In our study, most of the active phytocomponents of the investigated plants exhibited relative inhibitory potentials against Mpro of SARS-CoV-2 and preferred pharmacological features when compared with hydroxychloroquine. These findings indicate these compounds are potentially antiviral candidates against SARS-CoV-2.

Keywords: *Azadirachta indica*; *in silico*; *Mangifera indica*; *Moringa oleifera*; SARS-CoV-2 main protease

Introduction

Since the beginning of the 21st century, novel Coronaviruses (CoVs) have caused major outbreaks of fatal pneumonia globally.[1] Severe acute respiratory syndrome coronavirus (SARS-CoV) emerged and spread to five continents in 2003, while the Middle East respiratory syndrome coronavirus (MERS-CoV) broke out in the Arabian Peninsula in 2012. These outbreaks produced mortality rates of 10% and 35%, respectively.[1–5] However, both SARS-CoV and MERS-CoV are zoonotic viruses, and their hosts are bats or civets and dromedary camels, respectively.[6] To date, no specific therapeutic drug or vaccine has been approved for the treatment of human coronavirus; hence, human health is at significant risk due to the outbreaks of coronaviruses.[1]

In December 2019, several pneumonia cases emerged due to outbreak of an unprecedented coronavirus later called Severe Acute Respiratory Syndrome Coronavirus 2 (SARS-CoV-2) in Wuhan, China.[7–10] The whole genome of this novel coronavirus was sequenced, and it revealed that it is 96.2% identical to coronavirus in bats and possess 79.5% and <50% sequence similarities with SARS-CoV and MERS-CoV, respectively[1,11,12] The novel coronavirus was termed SARS-CoV-2 by the International Committee on Taxonomy of Viruses, and the associated pneumonia was designated as COVID-19 by World Health Organization (WHO) on February 11, 2020.[13] The disease not only spread rapidly to most provinces of China but also to over 200 countries and territories across all continents and was announced as a global health emergency by the WHO on March 11, 2020.[14]

The COVID-19 viral genome comprises approximately 30,000 nucleotides, and its replicase gene encodes two overlapping polyproteins, pp1a and pp1ab, essential for viral replication and transcription.[1,11,15] These functional polypeptides are then released from the polyproteins by extensive proteolytic cleavage, with the aid of a 33.8-kDa main protease (Mpro), alternatively called 3C-like protease and papain-like proteases (PLPs).[15] Biochemically, Mpro cleaves the polyprotein at 11 conserved sites to release non-structural proteins 4 to 16 (nsp4 - 16), starting with its self-cleavage from pp1a and pp1ab.[7,15,16] Interestingly, recent studies have highlighted the advantage linked to the identification of Mpro from SARS-CoV-2 as a target attractive for antiviral drug design due to the absence of related homologs of Mpro in humans.[7,15]

Regrettably, there are no specific therapies approved by recognized international health agencies, such as the WHO and US Food and Drug Administration (FDA) for SARS-CoV-2.[17–19] Presently, several agents, such as chloroquine,[20] hydroxychloroquine,[21] remdesivir,[22] lopinavir/ritonavir,[23] azithromycin,[24] and tocilizumab[25] are undergoing clinical trials under compassionate use protocols based on promising inhibitory effects exhibited against SARS-CoV-2 and related viral diseases*in vitro* is now a milestone for drug repurposing against this viral malady. Despite their success in clinical reports, none have gained approval for use against SAR-CoV-2 because their curative outcomes remain very limited and their toxic side-effects cannot be ignored. Conversely, a recent study from Xu et al.[19] and Ashfaq et al.[26] revealed the relevance of molecular docking techniques to find newer and potential inhibitors of Mpro. As such, alternative novel evidence based on the molecular docking approach could become useful for the advancement of novel drugs for the management and treatment of SARS-CoV-2.

Similarly, bioactive plant products play a key role in deterring disease and promoting treatment by enhancing antioxidant activity, inhibiting microbial growth, and modulating genetic pathways.[26–28] Also, the global interest in the health-promoting benefits offered by phytoconstituents has increased recently compared with other synthetic drugs is due to their cheap, ease of access coupled with their few side effects. Numerous pharmacologically active medications with minimal or no side effects are derived from natural sources, such as medicinal plants and microbes.[28] Furthermore, bioactive compounds from some plants possess antiviral activities.[29,30] Therefore, natural products possessing antiviral activity can be used as templates in the search for potential bioactive compounds against SARS-CoV-2. In this regard, molecular docking can predict the underlying mechanism, emphasizing the receptor protein interactions with bioactive compounds.

In recent years, *Azadirachta indica* (neem), an evergreen tree belonging to the family *Meliaceae,* has been regarded as an essential medicinal and fast-growing perennial tree found in Africa, America, and India. It has gained global significance due to its wide-ranging therapeutic activities.[26,31,32] It has considerable antinociceptive, emollient, antiviral, anti-inflammatory, antiseptic, antifungal, astringent, insecticidal, anti-helminthic, and antibacterial properties.[26,27,33] Over 140 active constituents with established therapeutic usefulness have been identified in various parts of this plant.[26] There are many constituents in *A. indica,* such as limonoids, nimbin, nimbidin, and nimbolide that can aid in disease management by

modulating numerous pathways of genetic relevance and other activities.[34] However, quercetin and β-sitosterol were the first polyphenolic flavonoids purified from fresh leaves of neem and were known to have antifungal and antibacterial activities.[27,31,34]

Mangifera indica of the *Anacardiaceae* family is one of the main tropical trees originating from Asia,[35] Brazil, China, India, Mexico, Nigeria, Pakistan, the Philippines, and Thailand, with India being the premier mango cultivating country.[36] Despite the common use of mango fruit as food, various parts of mango trees have also been used in folkloric medicine in most South-East Asian and African countries.[35,36] Barretto et al.[37] characterized and quantified a wide-range of polyphenolic compounds in *M. indica*. Mangiferin, gallic acid, catechins, quercetin, kaempferol, protocatechuic acid, ellagic acids, propyl and methyl gallate, rhamnetin, and anthocyanins are the major polyphenolic compounds found in *M. indica*.[36] According to Al Rawi et al.,[38] extracts from *M. indica* show antiviral activity against influenza virus H9N2 grown on cultured cells, with minimal cytotoxicity. Additionally, the bark, flowers, fruits, and leaves of *M. indica* have also been reported to possess antiviral properties.[35,36,39]

Another African plant, *Moringa oleifera* of *Moringaceae*, originates from northern India and can be cultivated in tropical and subtropical regions.[40–42] The diverse parts of the plant have traditional use in managing various ailments, such as arthritis, diabetes, fever, asthma, epilepsy, wounds, body pains and weakness, cough, blood pressure, skin infections, chronic anemia, cancer, viral infections, malaria, haemorrhage, tuberculosis, and other respiratory diseases.[43,44] Earlier reports revealed its inhibitory activity against a few infectious disease-causing viruses: human immunodeficiency, herpes simplex, hepatitis B, and Epstein–Barr.[40,43,44] *M. oleifera* possess a very high antioxidant activity.[40,45] In addition, the leaves are very rich in vitamins, carotenoids, polyphenols, phenolic acids, flavonoids, alkaloids, glucosinolates, isothiocyanates, tannins, saponins, oxalates, and phytates.[40,41,46]

Having considered the potential of these plant's bioactive compounds in the management and treatment of many diseases, with emphasis on their limitations, it is therefore essential to explore an evidenced-based molecular docking approach to assess the inhibitory potential of some of the active compounds from *A. indica, M. indica* and *M. oleifera* leaves against Mpro and also screen the top hit compounds for adsorption, distribution, metabolism, excretion, and toxicity (ADMET) *in silico*.

Materials and Methods

Protein target selection, preparation, and active site prediction

The three-dimensional (3D) X-ray crystal structure of Mpro found in SARS-CoV-2 (PDB ID: 6lu7) was obtained from the Protein Data Bank (PDB) (www.pdb.org/pdb). Using UCSF-Chimera© (version 1.13) software tools (http://www.cgl.ucsf.edu/chimera),[47] the protein target was prepared for docking by removing the co-crystallized ligand and additional water molecules to make it a nascent receptor, after which hydrogen charges were added to the protein. The DogSite module of the protein-plus web server (http://proteinsplus.zbh.uni-hamburg.de), which is based on the druggability score of identified pockets,[48] was applied to predict the binding site of Mpro.

Ligand preparations

Three-dimensional (3D) structures of the selected molecules were obtained in a simple data file from the PubChem server (https://www.ncbi.nlm.nih.gov/pccompound) and were converted to mole files using MarvinSketch© (ver. 15.11.30). The molecules were optimized for docking using the Merck molecular force field (MMFF94) in Avogadro (ver. 1.10). A total of twenty-two compounds from *A. indica, M. indica,* and *M. oleifera* was selected for the study, while hydroxychloroquine was adopted as a control drug.

Drug likeness screening

The selected compounds were screened for drug-likeness as described by Lipinski et al.[49] The compounds were analysed using DruLiTo software to predict their logP, molecular weight, and hydrogen bond donor and acceptor values. Lipinski's rule of five was applied to screen for the probable molecules that can serve as oral drugs.[50]

Validation of the in-silico docking protocol

The docking protocol was validated to substantiate the accuracy and reliability of the docking results, according to Gregory et al.[51] The goal was to accurately reproduce the binding pore and the molecular interactions of the co-crystallised ligand of the experimentally-crystallized protein structure. Accordingly, the native ligand of the x-ray protein was separated from the protein and then prepared for docking in UCSF-Chimera.[47] The ligand was then docked back into Mpro's active site using Auto Dock Vina in PyRx.[52] The docked complex was superimposed with the X-ray resolved crystal Mpro bearing the co-crystallized ligand to generate the root mean square deviation (RMSD) value in PyMOL. Notably, the RMSD value ranging from (0–2) Å is appropriate for docking and is indicative that the protocol could be subsequently used for other small molecule inhibitors.

In silico molecular docking

The docking was executed using a flexible docking protocol as described by Trott and Olson[52] with slight modifications. In brief, Python Prescription 0.8, a software suite of Auto Dock Vina, was utilized for the molecular docking analysis of the selected ligands with Mpro. The protein data bank, partial charge, and atom type (PDBQT) files of the protein were generated (using their previously created PDB files as inputs). The enzyme's target site was set with the help of a grid box with dimensions 27.601 Å × 32.911 Å x 32.182 Å, and the centres were

adjusted based on the active site of the enzyme. Once the molecular docking was completed, 10 configurations for each protein-ligand complex were generated for all the ligands. Text files of the scoring results were also created for manual comparative analysis. All through this *in silico* investigation, an exhaustiveness of 10 was used for docking to achieve results with high accuracy and reliability. The protein-ligand complexes as well the molecular interaction were all visualized in 3D and 2D using PyMOL© Molecular Graphics (version 1.3, 2010, Shrodinger LLC), LigPlot^{+}© Roman Lakoskwi, European Bioinformatics Institute, Hinxton, Cambridge, United Kingdom (version 2.1.), and the Protein-ligand interaction profiler's (PLIP) webserver (https://projects.biotec.tu-dresden.de/plip-web/plip) to check for additional interactions between the ligands and the Mpro.[53]

Prediction of ADMET properties

The ADMET properties of the compounds with the highest hits from the molecular docking studies were executed using the ADMETSar webserver (http://lmmd.ecust.edu.cn/).[54,55] This is a web platform in which the hit compounds were accessed for their aqueous solubility, pharmacodynamics, and pharmacokinetic properties using the various models.

Results

In this *in silico* study, 22 active compounds from the study plants and the control drug (Figure 1) were assessed for their inhibitory properties against Mpro (Figure 2) of SARS-CoV-2, the key protein implicated in the pathogenesis of COVID-19. Furthermore, the active site of Mpro was predicted using the DogSite scorer on the protein-plus web server, which is a fully automatic algorithm for predicting pockets and their druggability.[48] The higher the drug score of a predicted pocket, the more suitable it is for adoption as the binding site of a target protein. At the end of the prediction, 37 amino acid residues were identified in the pocket with the highest drug score and simple score. The amino acid residues are; Gln19, Thr25, Thr26, Leu27, Asn28, Arg40, His41, Cys44, Asp48, Met49, Pro52, Tyr54, Cys117, Tyr118, Asn119, Gly120, Phe140, Leu141, Asn142, Gly143, Ser144, Cys145, His163, His164, Met165, Glu166, Leu167, Pro168, His172, Phe181, Val186, Asp187, Arg188, Gln189, Thr190, Ala191 and Gln192. The platform predicted 24 out of the established 25 amino acids from previous studies.[1,15]

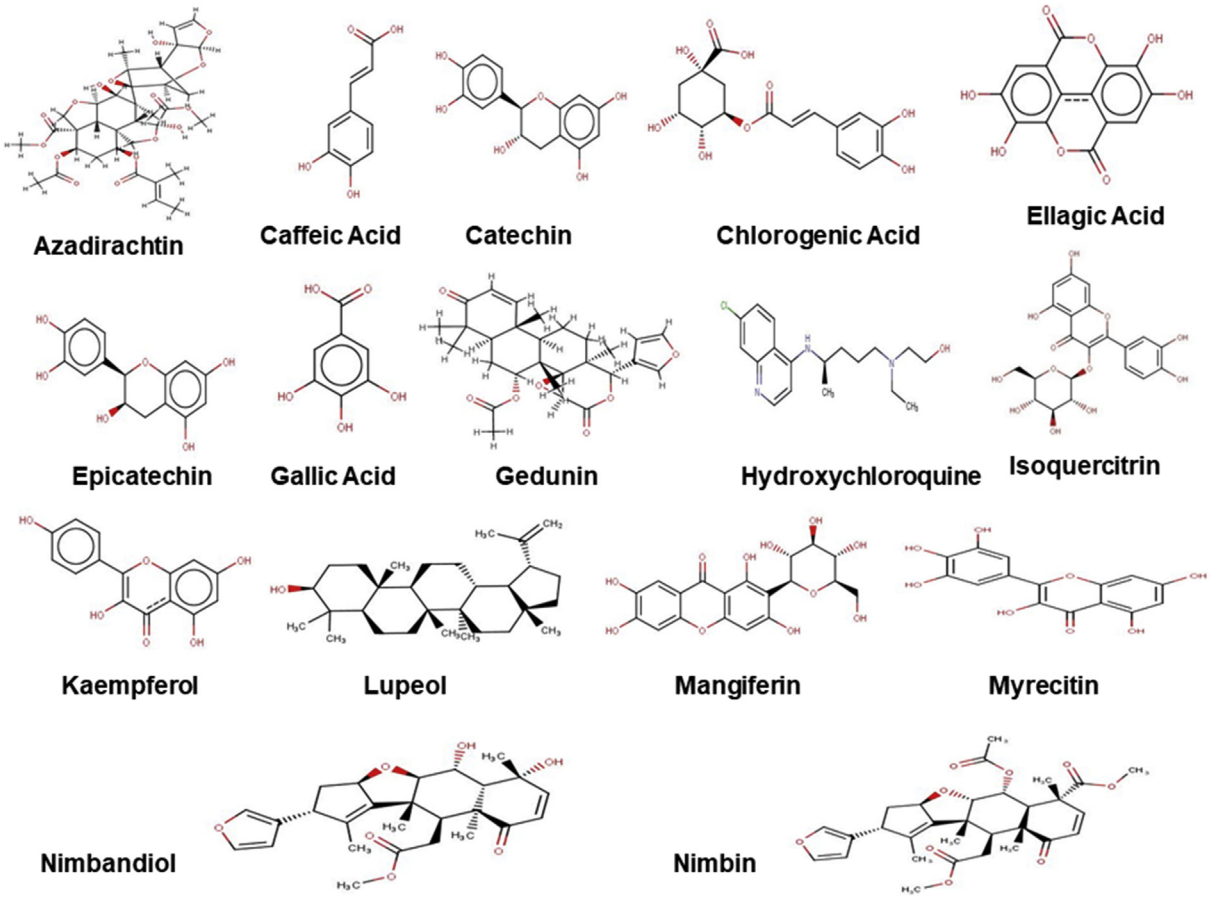

Figure 1: The structures of active compounds from *Azadirachta indica, Mangifera indica,* and *Moringa oleifera,* and the control drug (hydroxychloroquine).

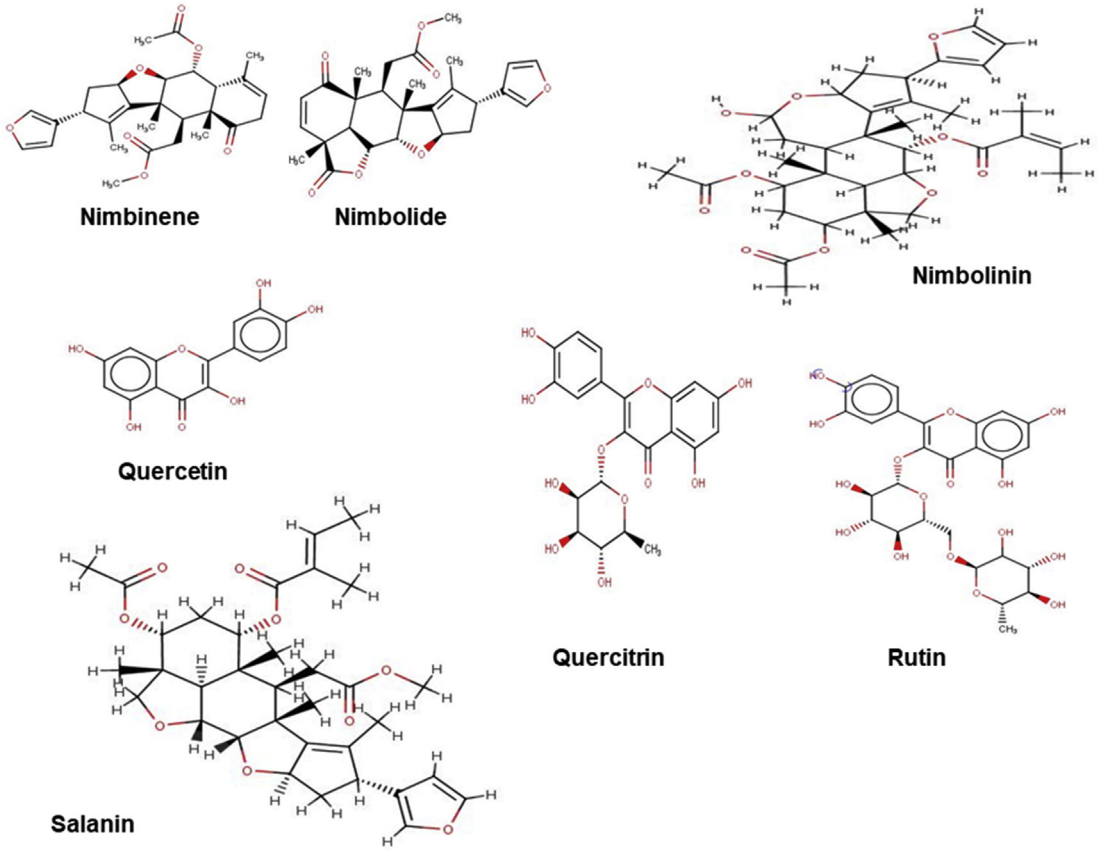

Figure 1: (*Continued*).

A total of 17 out of the 22 active compounds initially selected for this study passed Lipinski's rule of five. In contrast, the other five (azadirachtin, isoquercitrin, quercitrin, rutin, and salanin) that violated at least two of the rules were eliminated from further investigations (Table 1). Before docking, the protocol for docking was validated[51] as elucidated in the methodology. This process was carried out to provide assurances of the deployed protocols and docking tools to accurately provide correct binding signatures with quality interactions between the target protein and the bioactive compounds investigated in this study. This experiment was considered successful since the docked complex precisely reproduced the original pose as the native ligand (N-leucinamide) (Figure 3) with an RMSD value of 1.049 Å. The results of molecular docking between the assessed active compounds and Mpro is presented in Table 2. The docking outputs revealed that catechin, chlorogenic acid, ellagic acid, epicatechin, gedunin, kaempferol, lupeol, mangiferin, myricetin, nimbandiol, nimbinene, nimbolide, and quercetin had better binding positions with Mpro than with hydroxychloroquine, as adjudged by their relatively lower binding energy values (also see Figure 4). The control drug, hydroxychloroquine, has a binding energy of −6.4 kcal/mol while forming hydrogen bonds with Ser144, Cys145, Gln189 and Thr190 in the active site of Mpro, and it established a hydrophobic interaction with Phe140, Leu141, Asn142, Gly143, Ser144, Met165, Glu166, Arg188, and Gln189 in the active site of Mpro. Based on the docking outputs, mangiferin had the best binding position, with a binding energy of −8.4 kcal/mol. It interacts with the target enzyme to yield hydrogen bonds with nine amino acid residues in the active site of Mpro: His41, Leu141, Asn142, Gly143, Ser144, Cys145, Arg188, Thr190, and Gln192. Furthermore, it establishes hydrophobic interactions with His41, Met49, Leu141, Asn142, Gly143, Ser144, Cys145, Met165, Glu166, Arg188, Gln189, Thr190, and Gln192 in the Mpro active site. Conversely, gallic acid had the lowest binding affinity compared with other screened compounds and our control drug, as predicted from its relatively higher binding energy (−5.5 kcal/mol) after it was docked against Mpro. Gallic acid formed hydrogen bond interactions with Leu141, Gly143, Ser144, Cys145, His163 and Glu166 in the active site of Mpro and hydrophobically interacted with Mpro by binding with Phe140, Leu141, Asn142, Gly143, Ser144, His163, Met165, and Glu166 amino acids in the active cavity of the target protein. The relatively higher binding energy exhibited by

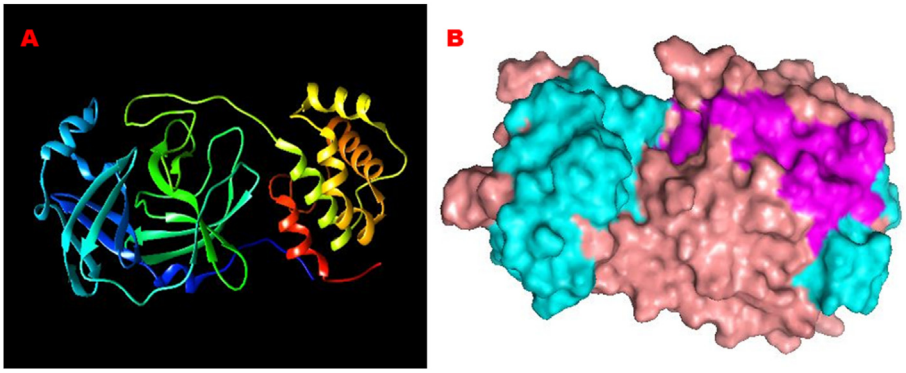

Figure 2: The structure of the ribbon pattern (a) and surface presentation, (b) of the main protease from SARS-CoV-2.

Table 1: Lipinski's drug-likeness screening of the control drug and the active compounds from *Azadirachta indica*, *Mangifera indica*, and *Moringa oleifera* leaves.

S/N	Plant	Phytochemicals	Chemical formulae	Molecular weight	LogP	Number of HB acceptor	Number of HB donor	No of violation
1	*Azadirachta indica*	Azadirachtin	$C_{35}H_{44}O_{16}$	720.26	−0.683	16	3	2
		Gedunin	$C_{28}H_{34}O_7$	482.23	3.557	7	0	1
		Nimbandiol	$C_{26}H_{32}O_7$	456.21	−0.311	7	2	0
		Nimbin	$C_{30}H_{36}O_9$	540.24	1.276	9	0	1
		Nimbinene	$C_{28}H_{34}O_7$	482.23	0.928	7	0	0
		Nimbolide	$C_{27}H_{30}O_7$	466.2	1.035	7	0	0
		Nimbolinin	$C_{35}H_{46}O_{10}$	626.31	3.137	10	1	1
		Salanin	$C_{34}H_{44}O_9$	596.3	3.089	9	0	1
		Quercetin	$C_{15}H_{10}O_7$	302.04	1.834	7	5	0
2	*Mangifera indica*	Catechin	$C_{15}H_{14}O_6$	290.08	0.852	6	5	0
		Ellagic acid	$C_{14}H_6O_8$	302.01	1.366	8	4	0
		Epicatechin	$C_{15}H_{14}O_6$	290.08	0.852	6	5	0
		Gallic acid	$C_7H_6O_5$	170.02	0.964	5	4	0
		Kaempferol	$C_{15}H_{10}O_6$	286.05	1.486	6	4	0
		Lupeol	$C_{30}H_{50}O$	426.39	11.901	1	1	1
		Mangiferin	$C_{19}H_{18}O_{11}$	422.08	−0.631	11	8	2
		Quercetin	$C_{15}H_{10}O_7$	302.04	1.834	7	5	0
		Rutin	$C_{27}H_{30}O_{16}$	610.15	−0.735	16	10	3
3	*Moringa oleifera*	Caffeic acid	$C_9H_8O_4$	180.04	0.888	4	3	0
		Catechin	$C_{15}H_{14}O_6$	290.08	0.852	6	5	0
		Chlorogenic acid	$C_{16}H_{18}O_9$	354.1	−0.7	9	6	1
		Ellagic acid	$C_{14}H_6O_8$	302.01	1.366	8	4	0
		Epicatechin	$C_{15}H_{14}O_6$	290.08	0.852	6	5	0
		Gallic acid	$C_7H_6O_5$	170.02	0.964	5	4	0
		Isoquercitrin	$C_{21}H_{20}O_{12}$	464.1	0.099	12	8	2
		Kaempferol	$C_{15}H_{10}O_6$	286.05	1.486	6	4	0
		Myrecitin	$C_{15}H_{10}O_8$	318.04	2.182	8	6	1
		Quercetin	$C_{15}H_{10}O_7$	302.04	1.834	7	5	0
		Quercitrin	$C_{21}H_{20}O_{11}$	448.1	0.802	11	7	2
		Rutin	$C_{27}H_{30}O_{16}$	610.15	−0.735	16	10	3
4	Control Ligand	Hydroxychloroquine	$C_{18}H_{26}ClN_3O$	335.18	1.548	4	2	0

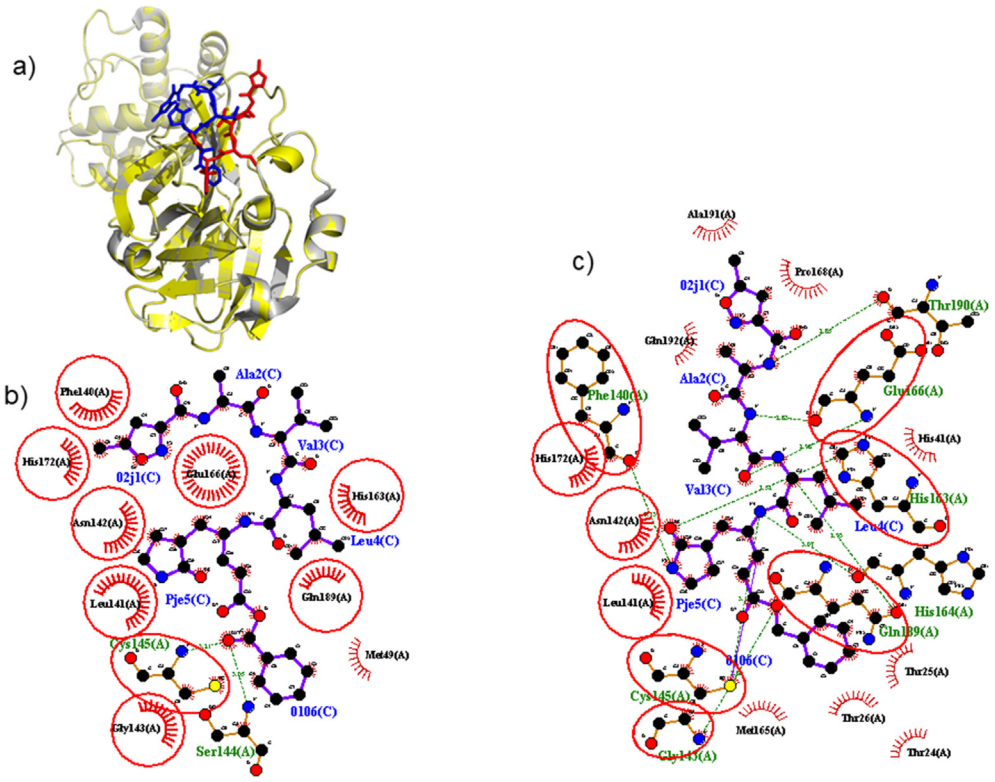

Figure 3: Molecular docking protocol validation. This crucial process can enhance the accuracy and reliability of an *in-silico* docking experiment. A comparison of the binding modes for the re-docked ligand (blue) vs. the co-crystallized ligand (red), shown as a stick representation. a) The molecular docking protocol accurately regenerated the binding configuration of a crystallographically determined protein-ligand complex with an RMSD value of 1.049 Å using PyMOL. Amino acid residue interactions with b) the re-docked and c) the co-crystallized ligand executed in LigPlot^{+}.

gallic acid is equivalent to the lowest binding affinity compared with other compounds and the control drug. Thus, the available data from the pool of investigated active compounds suggest that mangiferin and gallic acid may possess the most and least inhibitory effect against SARS-CoV-2 Mpro, respectively.

ADMET properties were predicted using the pharmacokinetic parameters of the ADMETSar web server (http://lmmd.ecust.edu.cn/) for six candidate compounds with hydroxychloroquine (control) after a successful docking study (Table 3). All the hit compounds possessed low absorption in the intestine via Caco-2 permeability except hydroxychloroquine, which might be due to the molecular size, whereas all possessed higher human intestinal absorption. Only the control, lupeol, and nimbolide exhibited blood−brain barrier penetrating potential. They all exhibited high plasma protein binding rates that might affect their movement to the target site to exert pharmacological actions. Most of them (5) reside in mitochondria, and the remainder (2) are localized in lysosomes. For drug metabolism, none of the compounds would be metabolized by CYP2D6 except hydroxychloroquine, and none of them would likely inhibit CYP2D6. Kaempferol, myricetin, and quercetin display inhibition of CYP1A2, which might indicate liver metabolism inhibition, while kaempferol showed inhibition of CYP2C19 and 2C9. All compounds would serve as a substrate to CYP3A4 except myricetin. Kaempferol, myricetin, nimbolide, and quercetin would likely inhibit CYP3A4. All compounds were found to be toxic in the *Salmonella typhimurium* reverse mutation assay (AMES), a preliminary drug screening assay to analyse whether a drug can cause mutations in *Salmonella typhimurium*.[56,57] None were predicted to be carcinogenic. All were predicted to cause hepatotoxicity in humans except hydroxychloroquine and lupeol. Hydroxychloroquine and nimbolide are p-glycoprotein substrates, indicating their ability to release phosphate from adenosine triphosphate (ATP). All compounds show good aqueous solubility, which might be due to the number of hydroxyl groups in them. Only hydroxychloroquine and nimbolide could block human ether-a-go-go (herG), a potassium ion channel.

Table 2: The binding energies and molecular interaction profiles of the control drug and the active compounds from *Azadirachta indica*, *Mangifera indica*, and *Moringa oleifera* leaves against the main protease of SARS-CoV-2.

Ligands	Plant Source	Binding Energy kcal/mol	No. of H-Bond	Residues involved in Hydrogen bond	Residues involved in hydrophobic interaction	Residues involved in π-stacking	Residues involved in Salt Bridge
Caffeic acid	*M. oleifera*	−5.6	3	Leu141,Ser144 and His163	Phe140,Leu141,Asn142,Gly143, Ser144,Cys145,His163,Met165, Glu166 and Gln189	–	–
Catechin	*M. indica and M. oleifera*	−7.2	4	Glu166,Asp187,Thr190 and Gln192	His41,His164,Met165,Pro168, Asp187,Arg188,Gln189,Thr190 and Gln192	His41	–
Chlorogenic acid	*M. oleifera*	−7.2	5	Cys145,His163,Arg188, Thr190 and Gln192	Leu141,Asn142,Gly143,His163, His164,Met165,Glu166,His172, Arg188,Gln189 and Thr190	–	His41, His163 and His172
Ellagic acid	*M. indica and M. oleifera*	−7.3	3	His41,Arg188 and Thr190	His41,Cys145,His164,Met165, Glu166,Asp187 and Arg188	–	–
Epicatechin	*M. indica and M. oleifera*	−7.0	3	Ser144,His163 and Gln189	His41,Met49,Phe140,Leu141, His163,His164,Met165,Glu166, Asp187,Arg188 and Gln189	–	–
Gallic acid	*M. indica and M. oleifera*	−5.5	6	Leu141,Gly143,Ser144, Cys145,His163 and Glu166	Phe140,Leu141,Asn142,Gly143, Ser144,His163,Met165 and Glu166	–	–
Gedunin	*A. indica*	−7.3	1	Asn142	His41,Asn142,Gly143,Cys145, His164,Met165,Glu166,Pro168, Gln189 and Thr190	–	–
Hydroxy chloroquine	Control ligand	−6.4	4	Ser144,Cys145,Gln189 and Thr190	Phe140,Leu141,Asn142,Gly143, Ser144,Met165,Glu166,Arg188 and Gln189	–	–
Kaempferol	*M. indica and M. oleifera*	−7.8	3	Leu141,Ser144 and Gln189	Met49,Leu141,Cys145,His163, Met164,His165,Glu166,Asp187, Arg188 and Gln189	–	–
Lupeol	*M. indica*	−7.6	–	–	His41,Asn142,Gly143,Cys145, His164,Met165,Glu166,Leu167, Pro168,Gln189 and Thr190	–	–
Mangiferin	*M. indica*	−8.4	9	His41,Leu141,Asn142, Gly143,Ser144,Cys145, Arg188,Thr190 and Gln192	His41,Met49,Leu141,Asn142Gly 143,Ser144,Cys145,Met165,Glu166, Arg188,Gln189,Thr190 and Gln192	–	–
Myrecitin	*M. oleifera*	−7.7	–	–	Thr26,Leu27,His41,Met49,Tyr54, Gly143,Cys145,His164,Met165, Asp187,Arg188 and Gln189	–	–
Nimbandiol	*A. indica*	−7.1	2	Thr26 and Gly143	Thr25,Leu27,His41,Met49,Phe140, Leu141,Asn142,Gly143,Cys145, Gln166 and Gln189	–	–
Nimbin	*A. indica*	−6.2	2	Arg40 and Arg188	Arg40,Tyr54,Glu55,Met82,Asn84, Cys85,Gly179,Asn180,Phe181, Val186,Asp187 and Arg188	–	Arg41 and Arg188
Nimbinene	*A. indica*	−6.5	2	Asn142 and Gly143	Thr25,Thr26,Leu27, Met49,Phe140,Leu1 41,Asn142,Gly143, Cys145 and Gln189	–	–
Nimbolide	*A. indica*	−7.6	3	Glu55, Phe181 and Arg188	Arg40,Asn53,Tyr54, Glu55,Met82,Cys85, Asn180,Phe181, Val186 and Arg188	–	Arg40 and Arg188
Nimbolinin	*A. indica*	−6.2	1	Arg40	Arg40,Tyr54,Glu55, Met82,Asn84,Cys85, Asn180,Phe181, Phe185,Val186 and Arg188	–	Arg40 and Arg188
Quercetin	*A. indica, M. indica and M. oleifera*	−7.5	4	Leu141,Ser144, His163 and Gln189	His41,Met49,Phe140, Leu141,His163,Met165, Glu166,Asp187,Arg188 and Gln189	–	–

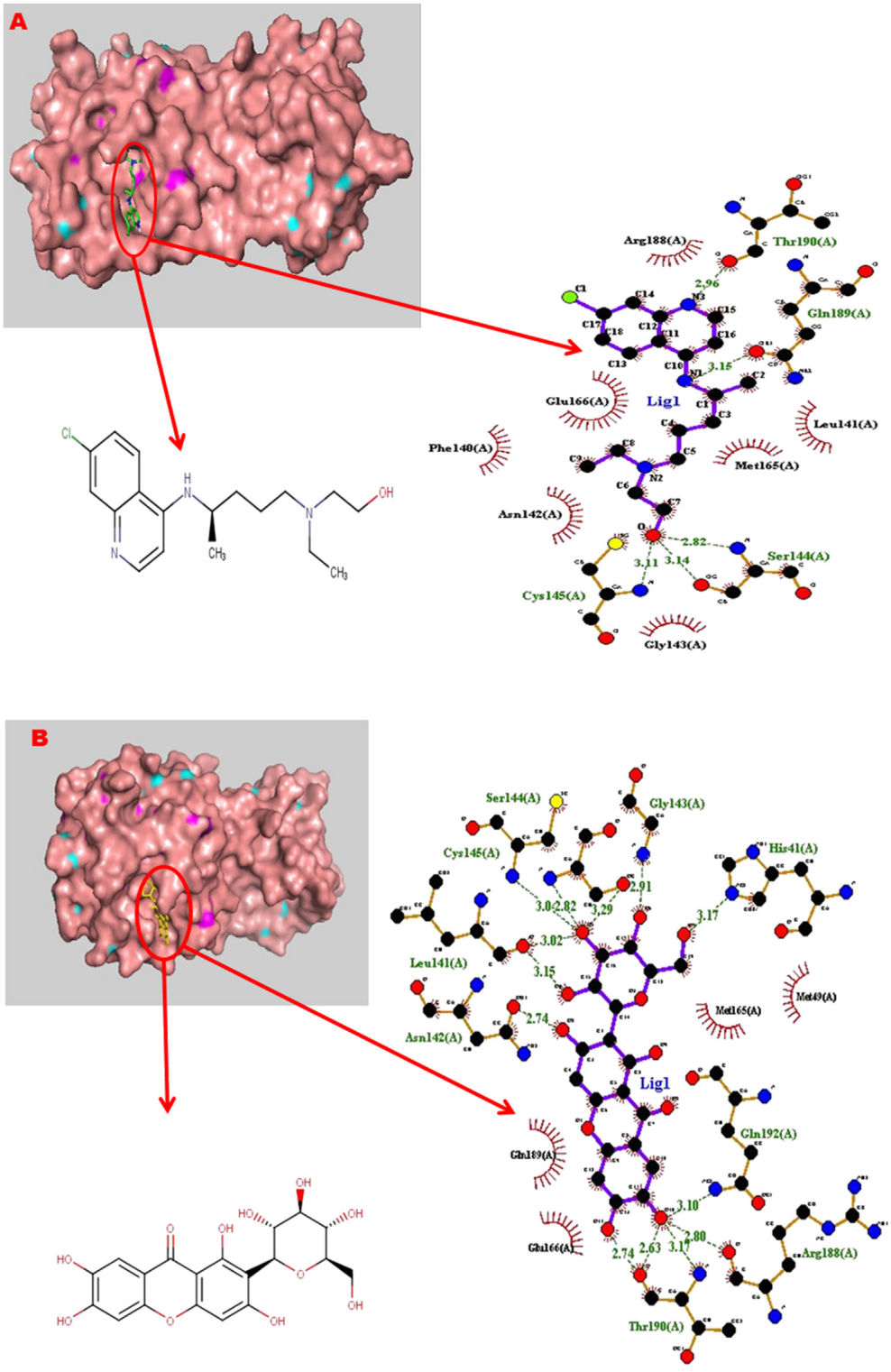

Figure 4: The binding configuration of ligands showing their poses and interactions in the binding site of the main protease of SARS-CoV-2. (a) Hydroxychloroquine, (b) mangiferin, (c) kaempferol, (d) lupeol, (e) nimbolide, and (f) quercetin. The interaction analysis shows hydrogen bonds (dashed green lines) and hydrophobic interactions (curved red lines) as ligands (purple) interact with the amino acid residues in the active site of Mpro.

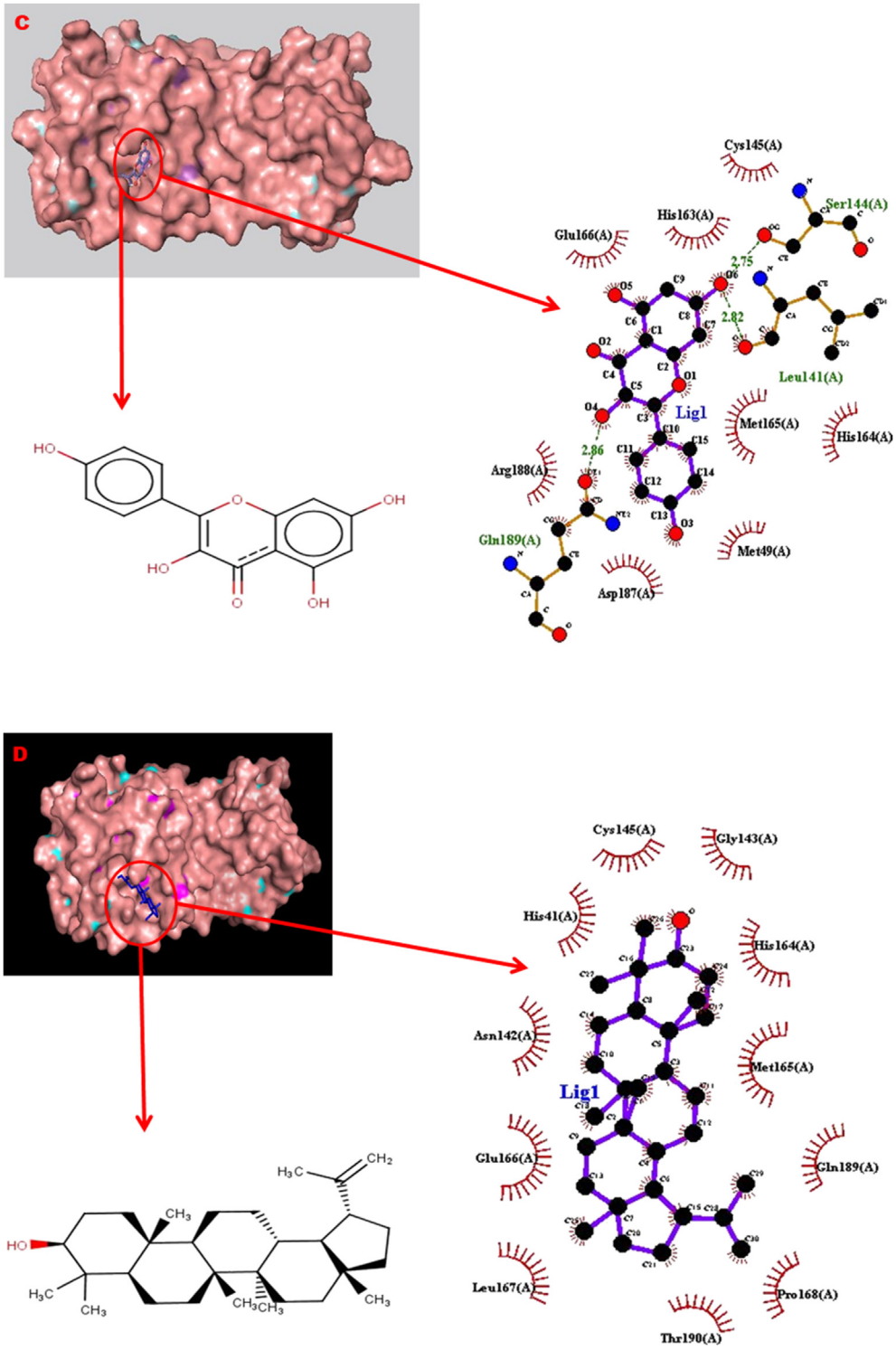

Figure 4: (*continued*).

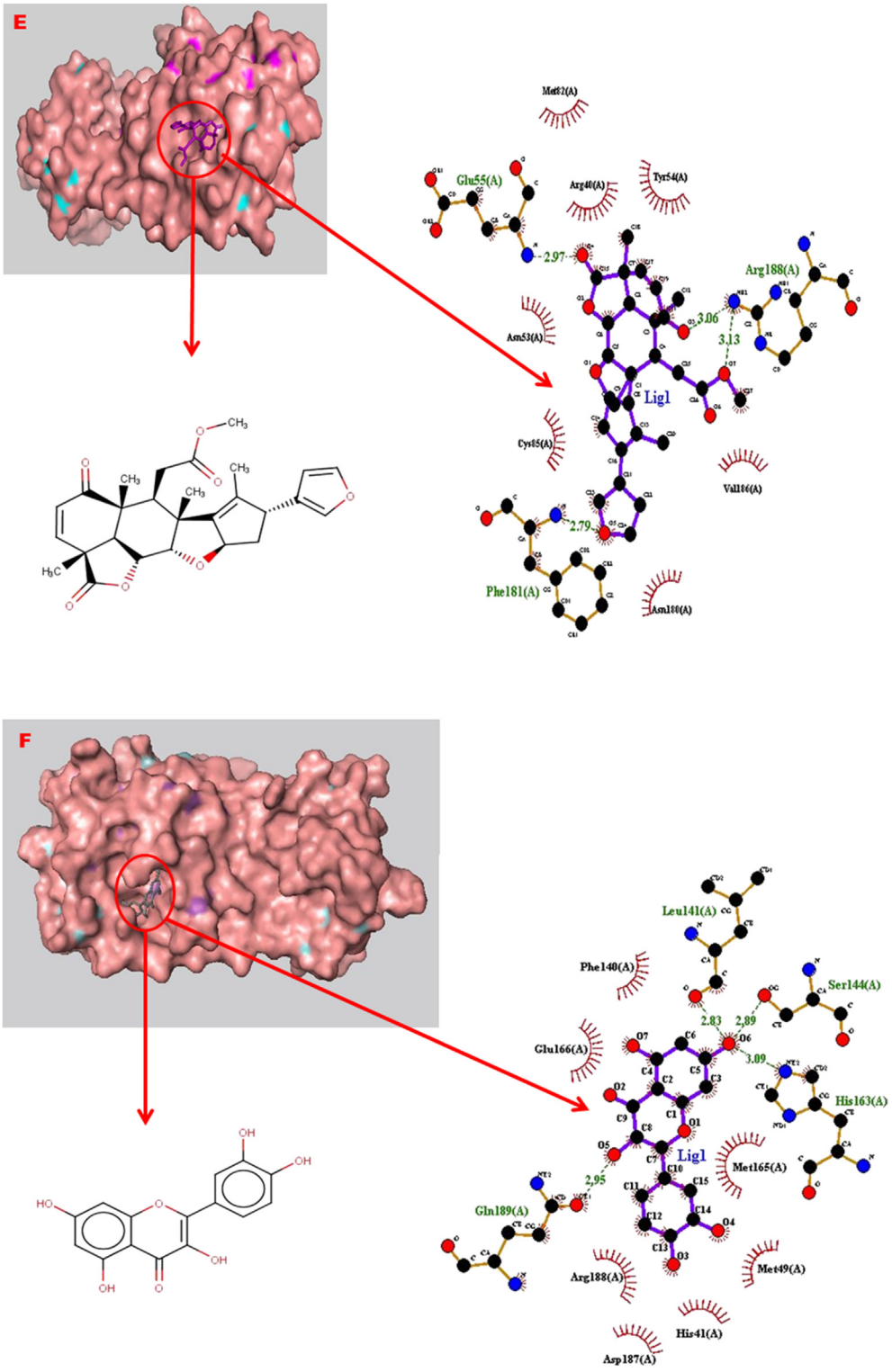

Figure 4: (*continued*).

Table 3: Absorption, distribution, metabolism, elimination, and toxicity predictions for kaempferol, mangiferin, myrecitin, nimbolide, and quercetin.

Models	Hydroxychloroquine	Kaempferol	Lupeol	Mangiferin	Myrecitin	Nimbolide	Quercetin
Ames mutagenesis	+	+	−	+	+	−	+
Acute Oral Toxicity (c)	III	II	III	IV	II	III	II
Blood Brain Barrier	+	−	+	−	−	+	−
Biodegradation	−	−	−	−	−	−	−
Caco-2 Permeability	+	−	−	−	−	−	−
Carcinogenicity	−	−	−	−	−	−	−
CYP1A2 inhibition	−	+	−	−	+	−	+
CYP2C19 inhibition	−	+	−	−	−	−	−
CYP2C9 inhibition	−	+	−	−	−	−	−
CYP2C9 substrate	−	−	−	−	−	−	−
CYP2D6 inhibition	−	−	−	−	−	−	−
CYP2D6 substrate	+	−	−	−	−	−	−
CYP3A4 inhibition	−	+	−	−	+	+	+
CYP3A4 substrate	+	+	+	+	−	+	+
CYP inhibitory promiscuity	−	+	−	−	+	+	+
Hepatotoxicity	−	+	−	+	+	+	+
Human either-a-go-go inhibition	+	−	−	−	−	+	−
Human Intestinal Absorption	+	+	+	+	+	+	+
Human oral bioavailability	+	−	−	−	−	−	−
Acute Oral Toxicity (Kg/mol)	2.6650	1.7388	3.8523	2.9792	2.3758	3.7769	2.5588
P-glycoprotein inhibitior	−	−	−	−	−	+	−
P-glycoprotein substrate	+	−	−	−	−	+	−
Plasma protein binding (100%)	0.7560	1.0613	1.0168	0.9697	1.1616	0.7761	1.1748
Subcellular localization	Lysosomes	Mitochondria	Lysosomes	Mitochondria	Mitochondria	Mitochondria	Mitochondria
UGT catalyzed	+	+	+	+	+	−	+
Water solubility Log*S*	−3.5660	−3.1423	−4.4139	−2.3978	−2.9994	−4.4552	−2.9994

Discussion

Lipinski's rule of five is a rule of thumb that evaluates a compound's drug-likeness to determine if the compound possesses specific biological or pharmacological activity conferring oral bioavailability in humans.[50] According to Usha et al.[56] and Singh and Konwar[57]; any compound that exceeds molecular weight (M_w) > 500 Da, calculated log P > 5, hydrogen-bond donors >5 and hydrogen-bond acceptors >10 is unlikely to be further pursued as a potential oral drug because it would likely be deficient in properties essential for the absorption, distribution, metabolism, and excretion.

According to Liu and Wang,[58] dozens of proteins are coded by the coronavirus, some of which are involved in viral replication and entry into cells. Mpro is an essential enzyme for coronaviral replication, making it an ideal target for drug design and development since humans do not possess a homologue. This enzyme's role is to cleave polyproteins 1a and 1 ab at 11 conserved sites to generate non-structural proteins 4 to 16 (nsp4-16), starting by self-cleavage (nsp5).[7,15,16] The Mpro adopted for this study was retrieved in its 3-D crystal structure (6LU7), co-crystallized with an N-leucinamide inhibitor with a resolution 2.16 Å, an amino acid sequence length of 306, and a homodimeric protein.[1,15] The catalytic site of Mpro consists of 25 amino acid residues after extensive literature mining vis: Thr25, Thr26, His41, Cys44, Met49, Tyr54, Phe140, Leu141, Asn142, Gly143, Ser144, Cys145, His163, His164, Met165, Glu166, Pro168, His172, Phe185, Val186, Asp187, Arg188, Gln189, Thr190, and Gln192. Also, the active site exhibits a *CysHis* (Cys145 and His41) catalytic dyad.[1,15] *In vitro and in vivo* studies on mangiferin, a C-glucosyl xanthone, have revealed various pharmacological activities that include antiviral properties.[35,36,59,60] The binding affinities between the active compounds (ligands) and Mpro in this study were stabilized by non-covalent interactions, such as hydrogen bonds, hydrophobic bonds, pie−stack interactions, and salt bridge formation (Figure 3 and Table 3). Similarly, Mohapatra et al.[61] and Salentin et al.[53] reported that the binding affinity would be higher (binding energy will be lower) if ligand's ability to form hydrophobic interactions with hydrophobic amino acid residues in the binding site is higher. Stojanovic and Zari reported the significance of hydrophobic interactions in many systems with strong intermolecular forces.[62] This evidence could be responsible for the appreciable binding affinity of the active compounds docked against Mpro in this study. Interestingly, the influence of a hydrogen bond in stabilizing the molecular interaction between the ligands and the protein cannot be downplayed because of its critical roles in enzyme catalysis, protein-substrate, and protein-inhibitor complexes as well as structural stability of various biological molecules.[53,62] To this end, analysis of molecular interactions exhibited by the active compounds assessed in this study as judged by their binding energies, hydrogen bonding, and hydrophobic interactions, with the surrounding amino acids in the active pocket of Mpro,

revealed the positive impact of their ligand–protein complex status, invariably enhancing the inhibition of Mpro from SARS-CoV-2.

The purpose of performing ADMET screening of any chemical compound within the human body is to determine the pharmacological and pharmacodynamic properties of a candidate drug compound within the biological system. Mangiferin was predicted to have high plasma protein binding and not be a p-glycoprotein substrate. Thus, mangiferin might be transported to its target site in an effective dose. The aqueous solubility predicted for mangiferin might be because of the numerous hydroxyl groups found in its structure. The liver is the leading site of metabolism for various drugs and xenobiotic agents, making it highly vulnerable to harmful effects; hence, hepatotoxic effects resulting from drugs or xenobiotic metabolic processes may result in severe organ (liver) collapse and ultimately death.[63] However, our *in-silico* study results are insufficient to ascertain the efficacies of the studied plant compounds in the management of COVID-19. This is the major limitation associated with this study. Hence, there is a great need for further *in vitro* and *in vivo* studies and clinical trials to validate the study plants' inhibitory potentials against SARS-CoV-2 primary protease replication.

Conclusions

In conclusion, most of the active phytocomponents of the study plants exhibited relative inhibitory potentials against Mpro of SARS-CoV-2 and preferred pharmacological features when compared with hydroxychloroquine, making them potential antiviral candidates in the fight against COVID. However, there is a need for further studies to ascertain the efficacies of these active compound(s), as the inhibitory properties displayed in this study may present an appropriate first step in the development of novel drugs for the management or treatment of coronavirus.

Recommendations

Since the pandemic remains a major health crisis and no cure has been found, an urgent need for further studies to establish the efficacies of these active compound(s) as their inhibitory properties displayed may present an appropriate leading step in the repositioning, repurposing, and development of novel drugs for the management or treatment of SARS-CoV-2.

Source of funding

This research did not receive any specific grant from funding agencies in the public, commercial, or not-for-profit sectors.

Conflict of interest

The authors have no conflict of interest to declare.

Ethical approval

There are no ethical or financial issues, conflicts of interest, or animal experiments related to this research.

Authors' contributions

HIU and AA conceived and designed the study, conducted research, and collected and organized the data. SSJ and PTS analyzed and interpreted the data. TOJ and JBD wrote the initial and final drafts of the article. HIU and SSJ reviewed the final version of the manuscript submitted for publication. All authors provided logistical support and approved the final draft, and are accountable for the manuscript's content and similarity index.

References

1. Wu C, Liu Y, Yang Y, Zhang P, Zhong W, Wang Y, et al. Analysis of therapeutic targets for SARS-CoV-2 and discovery of potential drugs by computational methods. **Acta Pharm Sin B 2020**; 10(5): 766–788.
2. de Groot RJ, Baker SC, Baric RS, Brown CS, Drosten C, Enjuanes L, et al. Commentary: Middle east respiratory syndrome coronavirus (mers-cov): announcement of the coronavirus study group. **J Virol 2013**; 87(14): 7790–7792.
3. Zaki AM, Van Boheemen S, Bestebroer TM, Osterhaus AD, Fouchier RA. Isolation of a novel coronavirus from a man with pneumonia in Saudi Arabia. **N Engl J Med 2012**; 367(19): 1814–1820.
4. Cheng VC, Lau SK, Woo PC, Yuen KY. Severe acute respiratory syndrome coronavirus as an agent of emerging and reemerging infection. **Clin Microbiol Rev 2007**; 20(4): 660–694.
5. Lee N, Hui D, Wu A, Chan P, Cameron P, Joynt GM, et al. A major outbreak of severe acute respiratory syndrome in Hong Kong. **N Engl J Med 2003**; 348(20): 1986–1994.
6. Reusken CB, Haagmans BL, Müller MA, Gutierrez C, Godeke G-J, Meyer B, et al. Middle East respiratory syndrome coronavirus neutralising serum antibodies in dromedary camels: a comparative serological study. **Lancet Infect Dis 2013**; 13(10): 859–866.
7. Dai W, Zhang B, Jiang X-M, Su H, Li J, Zhao Y, et al. Structure-based design, synthesis and biological evaluation of peptidomimetic aldehydes as a novel series of antiviral drug candidates targeting the SARS-CoV-2 main protease. **Science 2020**; 368: 1331–1335.
8. Zhu N, Zhang D, Wang W. China novel coronavirus investigating and research team. A novel coronavirus from patients with pneumonia in China, 2019. **N Engl J Med 2020**; 382(8): 727–733.
9. Li Q, Guan X, Wu P, Wang X, Zhou L, Tong Y, et al. Early transmission dynamics in Wuhan, China, of novel coronavirus–infected pneumonia. **N Engl J Med 2020**; 382: 1199–1207.
10. Chan JF-W, Yuan S, Kok K-H, To KK-W, Chu H, Yang J, et al. A familial cluster of pneumonia associated with the

2019 novel coronavirus indicating person-to-person transmission: a study of a family cluster. **Lancet 2020**; 395(10223): 514–523.
11. Zhou P, Lou YX, Wang X, Hu B, Zhang L, Zhang W. A pneumonia outbreak associated with a new coronavirus of probable bat origin. **Nature 2020**; 579(7798): 270–273.
12. Lu R, Zhao X, Li J, Niu P, Yang B, Wu H, et al. Genomic characterisation and epidemiology of 2019 novel coronavirus: implications for virus origins and receptor binding. **Lancet 2020**; 395(10224): 565–574.
13. Gorbalenya A, Baker S, Baric R, de Groot R, Drosten C, Gulyaeva A, et al. Coronaviridae Study Group of the International Committee on Taxonomy of Viruses. The species severe acute respiratory syndrome-related coronavirus: classifying 2019-nCoV and naming it SARS-CoV-2. **Nat Microbiol 2020**; 2020: 3–4.
14. Cucinotta D, Vanelli M. WHO declares COVID-19 a pandemic. **Acta Biomed: Atenei Parmensis 2020**; 91(1): 157.
15. Jin Z, Du X, Xu Y, Deng Y, Liu M, Zhao Y, et al. Structure of M^{pro} from SARS-CoV-2 and discovery of its inhibitors. **Nature 2020**; 582: 1–5.
16. Hegyi A, Ziebuhr J. Conservation of substrate specificities among coronavirus main proteases. **J Gen Virol 2002**; 83(3): 595–599.
17. Smith T, Bushek J, LeClaire A, Prosser T. *COVID-19 drug therapy*. Elsevier; 2020.
18. Tallei TE, Tumilaar SG, Niode NJ, Fatimawali F, Kepel BJ, Idroes R, et al. Potential of plant bioactive compounds as SARS-CoV-2 main protease (Mpro) and spike (S) glycoprotein inhibitors: a molecular docking study. **Preprintsorg 2020**: 1–18.
19. Xu X, Han M, Li T, Sun W, Wang D, Fu B, et al. Effective treatment of severe COVID-19 patients with tocilizumab. **Proc Natl Acad Sci Unit States Am 2020**; 117(20): 10970–10975.
20. Gao J, Tian Z, Breakthrough Yang X. Chloroquine phosphate has shown apparent efficacy in treatment of COVID-19 associated pneumonia in clinical studies. **Biosci Trends 2020**; 14(1): 72–73.
21. Yao X, Ye F, Zhang M, Cui C, Huang B, Niu P, et al. In vitro antiviral activity and projection of optimized dosing design of hydroxychloroquine for the treatment of severe acute respiratory syndrome coronavirus 2 (SARS-CoV-2). **Clin Infect Dis 2020**; 71(15): 732–739.
22. Wang M, Cao R, Zhang L, Yang X, Liu J, Xu M, et al. Remdesivir and chloroquine effectively inhibit the recently emerged novel coronavirus (2019-nCoV) in vitro. **Cell Res 2020**; 30(3): 269–271.
23. Cao B, Wang Y, Wen D, Liu W, Wang J, Fan G, et al. A trial of lopinavir–ritonavir in adults hospitalized with severe Covid-19. **N Engl J Med 2020**; 382(19): 1787–1799.
24. Gautret P, Lagier J-C, Parola P, Meddeb L, Mailhe M, Doudier B, et al. Hydroxychloroquine and azithromycin as a treatment of COVID-19: results of an open-label non-randomized clinical trial. **Int J Antimicrob Agents 2020**; 56(1): 105949.
25. Dong L, Hu S, Gao J. Discovering drugs to treat coronavirus disease 2019 (COVID-19). **Drug Discov Ther 2020**; 14(1): 58–60.
26. Ashfaq UA, Jalil A, ul Qamar MT. Antiviral phytochemicals identification from Azadirachta indica leaves against HCV NS3 protease: an in silico approach. **Nat Prod Res 2016**; 30(16): 1866–1869.
27. Alzohairy MA. Therapeutics role of Azadirachta indica (Neem) and their active constituents in diseases prevention and treatment. **Evid Based Complementary Altern Med 2016**; 2016: 7382506.
28. Latif A, Ashiq K, Ashiq S, Ali E, Anwer I, Qamar S. Phytochemical analysis and in vitro investigation of anti-inflammatory and xanthine oxidase inhibition potential of root extracts of Bryophyllum pinnatum. **J Anim Plant Sci 2020**; 30(1): 219–228.
29. Hu Q-F, Zhou B, Huang J-M, Gao X-M, Shu L-D, Yang G-Y, et al. Antiviral phenolic compounds from Arundina gramnifolia. **J Nat Prod 2013**; 76(2): 292–296.
30. Calland N, Dubuisson J, Rouillé Y, Séron K. Hepatitis C virus and natural compounds: a new antiviral approach? **Viruses 2012**; 4(10): 2197–2217.
31. Lee J-W, Ryu HW, Park S-Y, Park HA, Kwon O-K, Yuk HJ, et al. Protective effects of neem (Azadirachta indica A. Juss.) leaf extract against cigarette smoke-and lipopolysaccharide-induced pulmonary inflammation. **Int J Mol Med 2017**; 40(6): 1932–1940.
32. Del Serrone P, Failla S, Nicoletti M. Natural control of bacteria affecting meat quality by a neem (Azadirachta indica A. Juss) cake extract. **Nat Prod Res 2015**; 29(10): 985–987.
33. Ilango K, Maharajan G, Narasimhan S. Anti-nociceptive and anti-inflammatory activities of Azadirachta indica fruit skin extract and its isolated constituent azadiradione. **Nat Prod Res 2013**; 27(16): 1463–1467.
34. Sadeghian MM, Mortazaienezhad F. Investigation of compounds from Azadirachta indica (neem). **Asian J Plant Sci 2007**; 6(2): 444–445.
35. Ediriweera MK, Tennekoon KH, Samarakoon SR. A review on ethnopharmacological applications, pharmacological activities, and bioactive compounds of Mangifera indica (mango). **Evid Based Complementary Altern Med 2017**; 2017: 6949835.
36. Nayan V, Onteru SK, Singh D. Mangifera indica flower extract mediated biogenic green gold nanoparticles: efficient nanocatalyst for reduction of 4-nitrophenol. **Environ Prog Sustain Energy 2018**; 37(1): 283–294.
37. Barreto JC, Trevisan MT, Hull WE, Erben G, De Brito ES, Pfundstein B, et al. Characterization and quantitation of polyphenolic compounds in bark, kernel, leaves, and peel of mango (Mangifera indica L.). **J Agric Food Chem 2008**; 56(14): 5599–5610.
38. Al Rawi A, Al Dulaimi H, Al Rawi M. Antiviral activity of Mangifera extract on influenza virus cultivated in different cell cultures. **J Pure Appl Microbiol 2019**; 13(1): 455–458.
39. Jyotshna, Khare P, Shanker K. Mangiferin: a review of sources and interventions for biological activities. **Biofactors 2016**; 42(5): 504–514.
40. Biswas D, Nandy S, Mukherjee A, Pandey D, Dey A. Moringa oleifera Lam. and derived phytochemicals as promising antiviral agents: a review. **South Afr J Bot 2020**; 129: 272–282.
41. Vergara-Jimenez M, Almatrafi MM, Fernandez ML. Bioactive components in Moringa oleifera leaves protect against chronic disease. **Antioxidants 2017**; 6(4): 91.
42. Abdull Razis AF, Ibrahim MD, Kntayya SB. Health benefits of Moringa oleifera. **Asian Pac J Cancer Prev APJCP 2014**; 15(20): 8571–8576.
43. Ohemu T, Agunu A, Olotu P, Ajima U, Dafam D, Azila J. Ethnobotanical survey of medical plants used in the traditional treatment of viral infections in Jos, plateau state, Nigeria. **Int J Med Aromatic Plants 2014**; 4(2): 74–81.
44. Popoola JO, Obembe OO. Local knowledge, use pattern and geographical distribution of Moringa oleifera Lam.(Moringaceae) in Nigeria. **J Ethnopharmacol 2013**; 150(2): 682–691.
45. Stohs SJ, Hartman MJ. Review of the safety and efficacy of Moringa oleifera. **Phytother Res 2015**; 29(6): 796–804.
46. Leone A, Spada A, Battezzati A, Schiraldi A, Aristil J, Bertoli S. Cultivation, genetic, ethnopharmacology, phytochemistry and pharmacology of Moringa oleifera leaves: an overview. **Int J Mol Sci 2015**; 16(6): 12791–12835.
47. Pettersen EF, Goddard TD, Huang CC, Couch GS, Greenblatt DM, Meng EC, et al. UCSF Chimera—a visualization system for exploratory research and analysis. **J Comput Chem 2004**; 25(13): 1605–1612.

48. Volkamer A, Kuhn D, Grombacher T, Rippmann F, Rarey M. Combining global and local measures for structure-based druggability predictions. **J Chem Inf Model 2012**; 52(2): 360–372.
49. Lipinski CA, Lombardo F, Dominy BW, Feeney PJ. Experimental and computational approaches to estimate solubility and permeability in drug discovery and development settings. **Adv Drug Deliv Rev 1997**; 23(1–3): 3–25.
50. Lipinski CA. Drug-like properties and the causes of poor solubility and poor permeability. **J Pharmacol Toxicol Methods 2000**; 44(1): 235–249.
51. Warren GL, Andrews CW, Capelli A-M, Clarke B, LaLonde J, Lambert MH, et al. A critical assessment of docking programs and scoring functions. **J Med Chem 2006**; 49(20): 5912–5931.
52. Trott O, Olson AJ. AutoDock Vina: improving the speed and accuracy of docking with a new scoring function, efficient optimization, and multithreading. **J Comput Chem 2010**; 31(2): 455–461.
53. Salentin S, Schreiber S, Haupt VJ, Adasme MF, Schroeder M. Plip: fully automated protein–ligand interaction profiler. **Nucleic Acids Res 2015**; 43(W1): W443–W447.
54. Cheng F, Li W, Zhou Y, Shen J, Wu Z, Liu G, et al. admetSAR: a comprehensive source and free tool for assessment of chemical ADMET properties. **J Chem Inf Model 2012**; 52: 3099–3105.
55. Yang H, Lou C, Sun L, Li J, Cai Y, Wang Z, et al. admetSAR 2.0: web-service for prediction and optimization of chemical ADMET properties. **Bioinformatics 2019**; 35(6): 1067–1069.
56. Usha T, Middha SK, Goyal AK, Karthik M, Manoj D, Faizan S, et al. Molecular docking studies of anti-cancerous candidates in Hippophae rhamnoides and Hippophae salicifolia. **J Biomed Res 2014**; 28(5): 406.
57. Singh SP, Konwar BK. Molecular docking studies of quercetin and its analogues against human inducible nitric oxide synthase. **SpringerPlus 2012**; 1(1): 69.
58. Liu X, Wang X-J. Potential inhibitors against 2019-nCoV coronavirus M protease from clinically approved medicines. **J Genet Genomics 2020**; 47(2): 119.
59. Du S, Liu H, Lei T, Xie X, Wang H, He X, et al. Mangiferin: an effective therapeutic agent against several disorders. **Mol Med Rep 2018**; 18(6): 4775–4786.
60. Jhaumeer Laulloo S, Bhowon M, Soyfoo S, Chua L. Nutritional and biological evaluation of leaves of Mangifera indica from Mauritius. **J Chem 2018**; 2018(6869294): 1–9.
61. Mohapatra S, Prasad A, Haque F, Ray S, De B, Ray SS. In silico investigation of black tea components on α-amylase, α-glucosidase and lipase. **J Appl Pharmaceut Sci 2015**; 5(12): 42–47.
62. Stojanovic S, Zaric SD. Hydrogen bonds and hydrophobic interactions of porphyrins in porphyrin-containing proteins. **Open Struct Biol J 2009**; 3(1).
63. Hari S. In silico molecular docking and ADME/T analysis of plant compounds against IL17A and IL18 targets in gouty arthritis. **J Appl Pharmaceut Sci 2019**; 9(7): 18–26.

How to cite this article: Umar HI, Josiah SS, Saliu TP, Jimoh TO, Ajayi A, Danjuma JB. In-silico analysis of the inhibition of the SARS-CoV-2 main protease by some active compounds from select African plants. J Taibah Univ Med Sc 2021;16(2):162–176.